Analytical and Bioanalytical Chemistry
https://doi.org/10.1007/s00216-020-02643-3

RESEARCH PAPER

Bioassay engineering: a combined label-free and fluorescence approach to optimize HER2 detection in complex biological media

Alberto Sinibaldi[1] · Andrea Doricchi[1] · Tommaso Pileri[1] · Matteo Allegretti[2] · Norbert Danz[3] · Peter Munzert[3] · Elena Giordani[2] · Patrizio Giacomini[2] · Francesco Michelotti[1]

Received: 25 February 2020 / Accepted: 3 April 2020

Abstract

We report on the combined label-free/fluorescence use of one-dimensional photonic crystals to optimize cancer biomarker detection in complex biological media. The optimization of the assay working parameters permits us to maximize the final response of the biosensor. The detection approach utilizes a sandwich assay, in which one-dimensional photonic crystals sustaining Bloch surface waves are modified with monoclonal antibodies in order to guarantee high specificity during biological recognition. The multiple outcomes generated by such optimization experiments permitted us to determine the effective capture efficiency and the repeatability of the immobilization process, which was estimated to be close to 5%. By exploiting the resolution of the fluorescence operation mode, we studied non-specific interactions in different blocking agents, different analyte diluting buffers, and diverse concentrations of the detection antibody. As a clinically relevant biomarker, we selected the transmembrane receptor tyrosine kinase HER2. HER2 regulates a variety of cell proliferation, growth, and differentiation pathways and its over-expression occurs in approximately 20–30% of breast cancer worldwide. As a final application, we transferred all the optimized working parameters to HER2 cancer biomarker assays in a complex biological environment. The label-free and fluorescence results obtained by analyzing MCF-7 (HER2 low positive) and 32D (HER2 negative) cell lysates demonstrate that we can successfully discriminate the two lysates.

Keywords Optical biosensing · Label-free and fluorescence biosensors · Photonic crystals · Bloch surface waves · HER2

Introduction

The analysis of cancer biomarkers has great potential in the identification of cancer-related molecules in a wide span of pathologies with the aim to improve early diagnosis as well as therapy monitoring. With this regard, optical immunoassays attracted increasing interest in the field of clinical immunology because they exhibited the following interesting features: high sensitivity, high selectivity, non-invasive operation, reliability, and rapid signal generation [1–3]. Thanks to the favorable combination of both the optical analysis and the high affinity of antibody-antigen interaction, optical immunoassays have experienced an extensive development as a diagnostic tool for the simultaneous quantification of biomolecules.

A typical immunoassay makes use of the so-called sandwich approach. First (bio-conjugation), specific capture antibodies are immobilized onto a solid (optical) surface, which is then blocked by passivation. In second step (detection), the surface binds the analyte and a second detection antibody, which is specific for a different analyte's epitope, is used to complete the sandwich and to introduce a signal-amplifying molecule that transduces binding into a readable signal. Such an amplification strategy can utilize different transduction mechanisms. Indeed, depending on the experimental needs,

Published in the topical collection *Advances in Direct Optical Detection* with guest editors Antje J. Baeumner, Günter Gauglitz, and Jiri Homola.

Electronic supplementary material The online version of this article (https://doi.org/10.1007/s00216-020-02643-3) contains supplementary material, which is available to authorized users.

✉ Alberto Sinibaldi
alberto.sinibaldi@uniroma1.it

[1] Department of Basic and Applied Science for Engineering, Sapienza University of Rome, Via A. Scarpa 16, 00161 Rome, Italy

[2] IRCCS Regina Elena National Cancer Institute, Via Elio Chianesi 53, 00144 Rome, Italy

[3] Fraunhofer Institute for Applied Optics and Engineering IOF, A. Einstein-Str. 7, 07745 Jena, Germany

Published online: 16 April 2020

researchers can implement biotin-avidin recognition systems [4], enzyme-mediated reactions [2, 5], and detection antibody directly or indirectly conjugated with either organic dyes [6, 7] or nanoparticles [8]. The three intermediate steps, capture antibody immobilization, analyte recognition, and detection antibody, can be tailored by varying the working conditions in order to obtain an optimized biosensor response.

Usually, the performance of the complete sandwich assay is heavily influenced by variables that are primarily associated with the bio-conjugation step, such as surface chemistry, composition of the immobilization buffer, and the selection of a proper passivation strategy.

In order to find the optimized conditions, one should test all possible combinations of variables in terms of factors (type of parameters) and levels (values of the parameters), obtaining the so-called full factorial design. Such an optimization procedure foresees to vary a single input parameter keeping the others constant and to monitor the related output. Such laborious approach is called one-factor-at-time (OFAT) method (multifactorial approach) [6]. In addition, OFAT method could be influenced by an incorrect evaluation of the initial conditions because the optimal level of a factor could vary depending on the level of other factors. More efficient strategies, i.e., design of experiments (DoE), explained by Montgomery [9] as a methodology to apply statistics in optimization procedures, are nowadays preferred to mere OFAT methods [10]. For example, in DoE strategies, only a subset of all possible combinations are experimentally tested following a statistical strategy that maximizes the possibility to find the optimum. Indeed, one of the most widely used DoE in quality engineering process is the Taguchi method [11] but its application in biological research is still underappreciated [12].

In this work, we made use of a modified OFAT strategy to optimize iteratively the variables of an immunoassay for the detection of the HER2\neu (HER2) breast cancer biomarker, where the initial parameter choices were deduced from our previous experimental results [7].

HER2 is a member of the epidermal growth factor receptor family. It regulates a variety of cell proliferation, growth, and differentiation pathways crucial to neoplastic transformation [13], and is the major cancer driver in a potentially aggressive (but now curable) molecular subset (the HER2 subtype) comprising 20–30% of all breast cancers [14]. Molecular diagnosis is placed by a combination of gene amplification and protein over-expression tests, and determines access for the patient to a rich arsenal of approved, highly effective drugs including small molecules, antibodies, and antibody-drug conjugates (ADC). HER2 protein tests to quantitatively estimate the degree of HER2 over-expression are of interest for at least two reasons: (a) they may be integrated into routine diagnostic procedures and the current standard of care; (b) amplification wanes as a result of adaptive negative selection to HER2 blockade, which may result in the exhaustion of the therapeutic effects of HER2 blockade [15]. Therefore, quantitative longitudinal HER2 monitoring is likely to become mandatory in future precision oncology approaches.

The optical technique used in this study is based on one-dimensional photonic crystals (1DPCs) sustaining Bloch surface waves (BSW) [16–18] to develop and to optimize HER2 detection protocols. As recently demonstrated by some of the authors, 1DPCs have the peculiarity to operate simultaneously in both a label-free (LF) and a fluorescence (FLUO) mode, with two different dynamic ranges [4, 7, 19]. For HER2 in a cell lysate complex matrix, the LF mode can attain the limit of detection $LoD_{LF} = 16$ ng/mL whereas the FLUO mode extends such a limit down to $LoD_{FLUO} = 0.3$ ng/mL [7].

The aim of the present work is the monitoring and OFAT optimization, with a single multimode technique and within the same assay, of the biomolecular interactions taking place during all the key steps constituting the HER2 immunoassay. The LF mode is used when the interactions involve binding of large quantities of proteins at the sensors' surface, namely during the bio-conjugation step. The FLUO mode is used when a lower limit of detection is needed, namely when characterizing non-specific interactions or recognition/detection at a low HER2 concentration.

By using such an approach, we determined the optimum capture antibody concentration and immobilization conditions, the best performing blocking agent, the optimum concentration of the detection antibody, and the role of the composition of the analyte buffer. Hence, the combined label-free/fluorescence operation modes provided by 1DPC biochips contributed to set up a robust and reliable basis in engineering HER2 detection assays. In summary, this work wants to detail some of the issues that bioassay developers are faced with, as well as some solutions for improved bioassay development and validation of HER2 detection in complex biological matrices.

Materials and methods

1DPC sensors' design, fabrication, and readout system

The 1DCP biochips used in the experiments were designed to sustain BSW in the visible range to operate with protein solutions in aqueous environment [20]. The biochips were obtained by depositing the 1DPC onto optical quality plastic substrates made of cyclic olefin copolymer (TOPAS 5013 LS) [www.topas.com] with a prism-shaped cross section allowing to operate in the attenuated total internal reflection (TIR) configuration (Kretschmann-Raether) [21]. Fabrication was carried out by plasma ion–assisted evaporation under high vacuum conditions by means of an APS904 coating system (Leybold Optics) [20]. Moreover, the 1DPC chip is equipped

with a two-component flow cell consisting of a hard polymer cover that can be clicked on it. Inside the flow cell, an elastomer defines the micro channel and guarantees the sealing and the connection with the fluidic handling system [22].

The structure of the 1DPC is based on two pairs of bilayers, each constituted by a high Ta_2O_5 and a low SiO_2 refractive index layers with a thickness of $d_H = 120$ nm and $d_L = 275$ nm, respectively. In order to improve the adhesion onto the TOPAS substrate, an additional layer of SiO_2 with thickness d_L was first deposited. The optimized 1DPC forecasts a further TiO_2/SiO_2 bilayer, with a thickness for the two layers of d_F = 20 nm (Fig. 1a) [20]. The complex refractive indices of the layers' materials were as follows: $n(SiO_2) = 1.474 + j5 \times 10^{-6}$, $n(Ta_2O_5) = 2.160 + j5 \times 10^{-5}$, $n(TiO_2) = 2.28 + j1.8 \times 10^{-3}$ at $\lambda_0 = 670$ nm [23].

The 1DPC biochips were read out, in either LF or FLUO mode, as shown schematically in Fig. 1b and c, respectively. For the sake of simplicity, we do not sketch all the optical components used to manage the light beams (for a complete description of the optical layout, one can refer to our precedent work [4, 19]). The system is based on cylindrical optics and can read out simultaneously several different regions aligned along a line over the imaged 1DPC biochip surface.

In the LF mode, the 1DPC biochip is illuminated through the integrated prism coupler in TIR conditions [4, 7, 19] by a TE polarized and focused laser beam at $\lambda_0 = 670$ nm and the reflected beam is Fourier imaged on a CCD detector. A typical LF angular reflectance spectrum recorded in one region is shown in Fig. 1d. The angular range sampled by the CCD is 2.9°. The 1DPC was designed, optimized, and fabricated to work at $\theta_{0,BSW} = 69°$ and the thin TiO_2 layer was tailored to get a narrow width and large depth of the resonant dip [23].

The distribution of the TE polarized BSW energy density calculated at λ_0 and in resonance conditions is shown in Fig. 1a (red curve). The BSW is confined at the interface between the 1DPC and the external medium, where the field decays exponentially with a penetration length $L_{pen} = 117$ nm. Such a strong localization of the BSW provides a very sensitive tool to follow refractive index changes in close proximity to the SiO_2 outer layer, resulting from protein binding events.

In the FLUO mode, the biochip is excited by a TE polarized and slightly focused laser beam at the wavelength λ_{EXC} = 635 nm, matching the absorption peak of the Alexa Fluor 647 dye selected for the assays. The angle θ_{EXC} is set so that resonant excitation condition of a BSW at λ_{EXC} is achieved, therefore enhancing the excitation intensity and giving rise to an increased fluorescence emission. Moreover, the dye fluorescence is channeled via the BSW modes, radiated into a narrow angular range through the substrate, and finally imaged by the CCD (Fig. 1c) [4, 19, 24]. A typical angular fluorescence intensity (F) spectrum recorded in a 8° angular range is shown in Fig. 1e. In the following sections, W is the angularly integrated F. In all measurements reported here, the background fluorescence intensity, due to either stray light from the excitation or fluorescence of the 1DPC, was always measured before the assays and subtracted from the final result.

Chemical functionalization of the 1DPC

Among all possible bio-conjugation strategies [25], here, we made use of a surface modification technique via (3-aminopropyl)triethoxysilane (APTES) and glutaraldehyde (GAH) covalent linkage [26, 27]. The bare BSW biochips were first cleaned in a piranha solution for 10 min, rinsed thoroughly with double-distilled water (DDW), and dried under a stream of air. The clean 1DPC chips were allowed to react with a 2% solution of APTES in a mixture of ethanol/water (95:5 v/v) at room temperature (RT) for 1 h. Then, they were immersed in ethanol, sonicated, dried under a stream of air, and baked on a hot plate at 110 °C for 1 h. Then, the APTES-modified chips were allowed to react with 1% (v/v) glutaraldehyde in 100 mM sodium bicarbonate buffer (pH 8.5) in the presence of 0.1 mM sodium cyanoborohydride

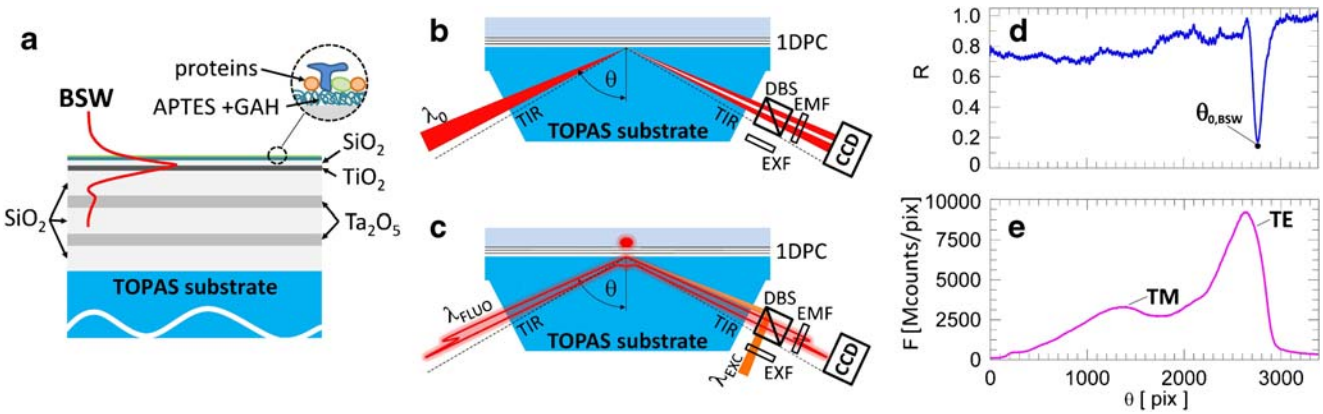

Fig. 1 (a) 1DPC geometry including functionalization chemistry (not to scale). Sketches of the label-free (b) and fluorescence (c) operation modes. (d) TIR angular reflectance profile, with the biochip in buffer (PBS 1×). (e) Fluorescence emission spectrum (F) at the end of the bioassay where HER2 was detected (violet curve); the TE and TM bands are also marked

for 1 h at RT. Lastly, after a second washing procedure in DDW, the glutaraldehyde-activated 1DPC biochips were complemented with the two-component fluidic cell and mounted on the optical readout system to be used in a cancer biomarker detection assay.

Cell biology and biochemistry

Three different cell lines were used in our experiments. The KPL-4 and MCF-7 breast cancer cells were used as a convenient source of HER2 molecules since they over-express or express at low level the HER2 gene. By contrast, the murine-derived hematopoietic cell line 32D was selected as a negative control because it lacks HER-kinases [28, 29]. Details on the cell lines growth and cell characterization are in the Electronic Supplementary Material (ESM, Section S1).

The monoclonal antibodies (mAbs) W6/300G9 (Anti-HER2) and W6/900 (detection Anti-HER2) were used to bind distinct epitopes of the HER2 ectodomain [30, 31]. In order to introduce fluorescence features, the detection Anti-HER2 was conjugated to the NHS ester of Alexa Fluor 647, at an approximate molar ratio of 10:1 to give a fluorescent detection antibody (Anti-HER2*). For the optimization experiments, we made use of the recombinant-HER2-Fc chimera (from R&D Systems). All mAbs were dissolved in phosphate-buffered saline 1× (PBS 1× , 10 mM). All the chemical reagents, i.e., sulfuric acid (95–98%), hydrogen peroxide (30% in H_2O), (3-aminopropyl)triethoxysilane (APTES, 99%), ethanol (99.8%), glutaraldehyde solution (grade I, 50% in H_2O), sodium bicarbonate (99.7%), sodium cyanoborohydride (95%), hydrogen chloride (2 M), glycine (99%), bovine serum albumin (BSA, 98%), and PBS 10× (100 mM), were purchased from Sigma-Aldrich. All blocking agents, human serum albumin (HSA), skimmed milk (SM), ethanolamine (MEA), and casein, were purchased from Sigma-Aldrich and were dissolved in PBS 1×. Alexa Fluor 647 NHS Ester (1 mg/mL) was purchased from Thermo Fisher Scientific.

Results and discussion

In this section, the optimization routes will be detailed in terms of the input parameters and levels chosen in the experiments. Once the optimization is carried out, such conditions will be transferred to a HER2 assay in a complex biological medium such as a cell lysate.

Bioassay format

In order to optimize the assay, two crucial steps must be addressed accurately. First, we must guarantee a high density of functional biological probes (bio-conjugation step). Second, we must tune the detection conditions to maximize the response (detection step). The detailed study of such two steps can generate via the OFAT approach those factors and levels that optimize the assays. Figure 2 shows the signal recorded in LF mode during the two steps of a typical assay reported herein. In the figure, we also mark the time when the FLUO measurements are carried out.

Figure 2a refers to the bio-conjugation step, which is constituted by the immobilization of the Anti-HER2 and the blocking procedure (BLK), each followed by a washing step in a simple buffer (pure PBS 1×, 5 min each). $\Delta\theta_{CAP}$ and $\Delta\theta_{BLK}$ are the residual LF signals in the buffer, in CCD camera pixels units, after either immobilization of Anti-HER2 or blocking, respectively. Making use of the calibrated sensitivity 16.5 pg/(mm^2 pix) in the LF mode and in linearity regime [22], the residual shifts (pixel) could be quantitatively converted to the surface density of the biomolecules (pg/mm^2) finally bound at the surface of the biochip. Moreover, the density and the refractive index of the protein layers show a clear dependence on the size of the molecules; proteins with larger molecular weight form a less dense layer whereas adsorbed small proteins relate to the formation of a more dense protein layer [32]. However, since here we are performing a comparison between the results obtained when changing factors and levels, dealing with the surface density or with the residual shift is equivalent. Therefore, in the following we keep the LF signal in pixel.

While the concentrations, the working conditions, and the blocking agents were matter of optimization, the working temperature $T = 30$ °C, the contact time of solutions $t = 15$ min., the flow rates $f_L = 1.3$ μL/s, and the volume of the samples injected $v = 160$ μL were kept constant during all the experiments.

Figure 2b refers to the detection step, which consists of the interaction with the analyte (HER2) solution and with the detection antibody (Anti-HER2*), followed in both cases by a washing procedure in running buffer (5 min)to remove the unbound excess proteins. $\Delta\theta_{HER2}$ and $\Delta\theta_{DET}$ are the residual LF signals in the buffer, in CCD camera pixels units, after either analyte recognition or detection with Anti-HER2*, respectively. Again, $T =$ 30 °C, $t = 10$ min, $f_L = 1.3$ μL/s, and $v = 160$ μL were the same for all detection experiments. Moreover, the fluorescence angular spectra were recorded before (background) and after (signal) the interaction with the labeled Anti-HER2* as indicated in Fig. 2b.

Capture antibody immobilization step

Figure 2a shows that the signal recorded in the LF mode allows to monitor and quantify in real time the Anti-HER2 immobilization process by directly relating the angular residual shifts to the amount of attached ligands.

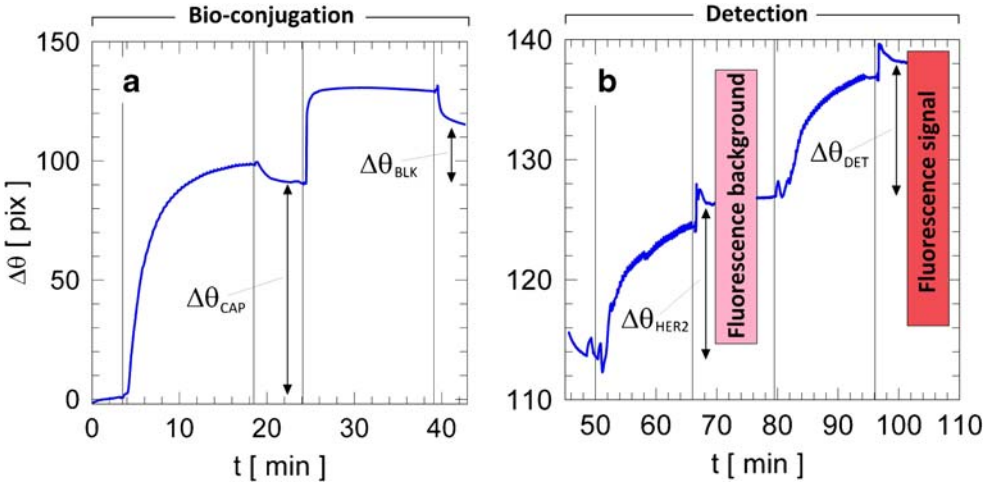

Fig. 2 LF sensorgrams of the (a) bio-conjugation and (b) detection steps. In the latter case, the time intervals when the FLUO measurements were also marked

Figure 3 reports the residual LF signals $\Delta\theta_{CAP}$, $\Delta\theta_{HER2}$, and $\Delta\theta_{DET}$ recorded in three different complete assays carried out with different biochips and by the same protocol. The only difference was the pH of the buffer in which the Anti-HER2 antibodies for the immobilization step were dissolved. We explored three pH values, 7.4, 8.5, and 9.6, including a pH value very close to the isoelectric point of the Anti-HER2 (pI = 8.6). In the assays, the concentrations of the bio-reagents were as follows: Anti-HER2 (0.1 mg/mL), BSA for blocking (1 mg/mL), HER2 (0.5 μg/mL), and Anti-HER2* (10 μg/mL). The running buffer was pure D-PBS 1× (10 mM).

The surface density of the Anti-HER2 after the immobilization procedure $\Delta\theta_{CAP}$, appears to be significantly increased at pH 7.4, with respect to the other two cases pH 8.5 and pH 9.6. We point out that the density of functional groups at the surface of the biochip after APTES and GAH chemistry, was checked to be almost constant, within 6% relative error (1std), by performing repetitive HER2 detection assays under the same conditions and with several different biochips (ESM, Fig. S2).

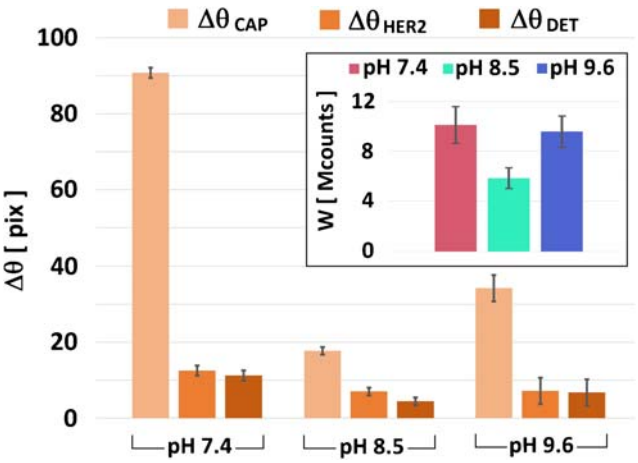

Fig. 3 LF residual shift related to the capture antibody immobilization ($\Delta\theta_{CAP}$) and detection assay steps ($\Delta\theta_{HER2}$, $\Delta\theta_{DET}$) in three different pH immobilization conditions for the capture antibody (pH = 7.4, 8.5, 9.6). The residual shift was averaged on 7 spots along the 1DPC biochip surface. The error bar corresponds to the standard deviation calculated over 7 sensorgrams at the end of the washing procedure. Inset: background subtracted integrated fluorescence for the three pH cases

Therefore, the differences observed for $\Delta\theta_{CAP}$ are effectively due to the pH and not to the starting conditions of the biochip. Such differences were transferred through the two subsequent steps of the bioassay, in terms of $\Delta\theta_{HER2}$ and $\Delta\theta_{DET}$, respectively. For all pH cases, $\Delta\theta_{HER2}$ and $\Delta\theta_{DET}$ were always comparable proving that a 1 to 1 interaction occurred, as expected for such a biological interaction model [31]. The inset of Fig. 3 shows that the FLUO intensities, which are proportional to the total amount of Anti-HER2* finally bound at the surface, confirmed the behavior obtained for $\Delta\theta_{DET}$ in LF, showing a slight prevalence of the case pH 7.4 as well.

It is worth observing that in Fig. 3, the marked difference between the $\Delta\theta_{CAP}$ values recorded for pH 7.4 and 9.6 (57 ± 3.7 pix) does not match the observation of comparable values, within the limit of the errors, for $\Delta\theta_{HER2}$ (5.3 ± 3.7 pix). On the other hand, the FLUO signals shown in the inset of Fig. 3, which are proportional to the total amount of Anti-HER2* finally bound at the surface, confirm such observation with a better confidence, with a slight prevalence of the case pH 7.4. Such a result could be ascribed to a better orientation and capture efficiency of less densely packed capture Anti-HER2 on the biochips prepared at pH = 9.6.

Based on the results of Fig. 3 and following the suggestion by Whitesides et al. [33] to use pH value 1 point below the pI of the antibody to be immobilized, we selected pH = 7.4 as the working condition for all subsequent assays.

In addition, further assays were carried out by varying the concentration of Anti-HER2 solution (5, 25, and 100 μg/mL) during the immobilization (ESM, Fig. S3). The results of the analysis demonstrated that the largest Anti-HER2 concentration that was tested (100 μg/mL) guarantees an optimal number of receptors linked at the surface.

Passivation step

Five different molecules were tested to block the surface to for prevent non-specific interactions: BSA, HSA, MEA, SM, and casein. Five different 1DPC biochips were prepared within the same functionalization batch until the GAH step and then exposed to the five different blocking agents, with the aim to investigate the resulting different degree of passivation. Then, all biochips were used with the same standard bioassay detection protocol (HER2 and Anti-HER2*). In agreement with their ideally inert nature, the sensorgrams recorded in the LF mode for all five 1DPC biochips did not show any significant residual angular shift (not shown here), within the limited resolution provided by the LF mode. However, by exploiting the better resolution of the FLUO mode, we could measure reliable FLUO signals and rank the blocking agents. Figure 4a shows the integrated fluorescence *W* values, obtained as the mean over seven different spots, for all five blocking agents. The results show that passivation with SM, casein, and BSA provided the three lowest *W* values and thus are better suited for blocking.

However, the success of a passivation strategy can be influenced dramatically by the specific recognition protocol that is used after the blocking step. As an example, the streptavidin-biotin interaction has been successfully used in a number of applications including the detection of proteins, nucleic acids, and lipids as well as protein purification [www.rockland-inc.com]. It is used routinely to link proteins in immunoassays by exploiting the very high affinity of such an interaction and we wish to preserve the possibility of using it in our protocols. With this in mind, despite their better blocking capability, SM and casein should be avoided because of their residual biotin content, which could interfere with the assay.

As a consequence, when biotinylated Anti-HER2* were used, we selected 0.1% BSA as a blocking agent, as also supported by the literature that identifies 0.1–2.0% BSA fraction V as a valid approach [www.rockland-inc.com]. In the case of the cancer biomarker detection assay we show below, in which we made use of Anti-HER2* directly conjugated to a dye, SM is the preferable option and was therefore used for blocking.

Analyte buffer

By keeping the bio-conjugation and detection assay parameters fixed, we dissolved a concentration of 0.1 μg/mL of HER2 in three different buffers: PBS 1×, a BSA solution of 1 mg/mL in PBS 1×, and the same solution adding a 0.05% of Tween 20. In this case, we directly compare the FLUO signal levels. Figure 4b plots the integrated fluorescence intensities (*W*) as a function of the three different diluting buffers compared with the blank signal. The blank was measured by using same protocol parameters except for the HER2 injection, which was replaced by 0.1% solution of BSA in PBS 1×. The three *W* values (Fig. 4b) were comparable with a slight prevalence for the PBS 1× and BSA cases. The addition of the 0.05% of Tween 20 to the BSA buffer intended to prevent sticking of proteins on tubing and fluidic cell but did not improve the final response, contrarily to what is expected. Therefore, in all experiments in which the HER2 analyte is spiked in a buffer, we made use of PBS 1×. In experiments with lysates, the dilution buffer was the lysis buffer.

Detection step

An additional study on the influence of the Anti-HER* concentration on the detection assay was also carried out. The Anti-HER2* was directly conjugated with an Alexa Fluor

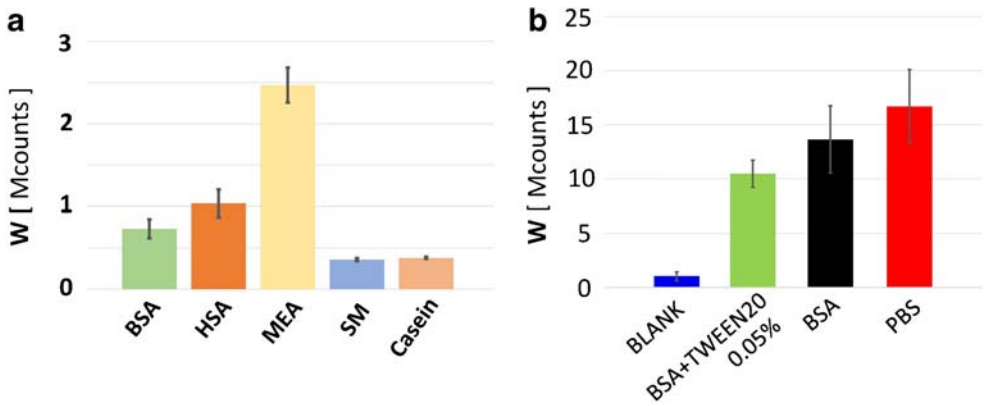

Fig. 4 (a) Integrated fluorescence intensities for five different passivation routes on 1DPC biochips; (b) integrated fluorescence intensities as a function of three different HER2 diluting buffers: PBS 1× (red curve), BSA solution (dark curve), and BSA with 0.05% of Tween 20 (green curve). As a reference, we reported the *W* of the blank (blue curve). In both cases, the fluorescence spectra were averaged on 7 spots, while the error bars represent the standard deviation

647 and used in the assay. Adopting the optimized bio-conjugation conditions and keeping the HER2 concentration constant ($c = 0.5$ μg/mL), we varied the Anti-HER2* concentration. As shown in Fig. 5a, the FLUO signal W at the end of a complete assay increases when increasing the Anti-HER2* concentration. The fluorescence signal saturates within the experimental error at concentrations above 5 μg/mL.

On the other hand, in assays carried out by means of fluorescence-activated cell sorting (FACS), we found that a large Anti-HER2* concentration increases the contribution of non-specific interactions as well as the fluorescence background. In Fig. 5b and 5c, we show the results of the FACS assays carried out with selected HER2-negative (32D) and HER2-positive (KPL-4) cell lines for increasing concentration, from 1 to 10 μg/mL, of the same Anti-HER2*. In both cases, the FACS are compared with a reference cell line (gray shadow curve). Figure 5a confirms what observed with the 1DPC biochips: for the KPL-4 positive line, with concentrations larger than 1 μg/mL, the number of counts, i.e., the detection efficiency, is almost constant and well separated from the reference. Contrarily, Fig. 5c shows that the non-specific signal recorded for the negative line scales with the Anti-HER2* concentration, therefore giving rise to an increasing non-specific signal.

Such considerations therefore suggest to use a concentration of Anti-HER2* in the range of (1 ÷ 2.5) μg/mL, which by the way also matches the recommendations of the suppliers of ELISA kits for HER2 detection based on different proprietary capture and detection antibodies [www.rndsystem.com].

Optimized HER2 assays in cell lysates

After optimizing all intermediate steps of the protocol, the bio-conjugation and detection parameters were implemented in a 1DPC biochip assay for the detection of HER2 in a complex biological medium. As a biological source of HER2, we made use of two different lysates from cell lines: MCF-7 (low HER2 expression) and 32D (HER2 negative, used as reference) [28, 29]. The two lysates were ranked by Western blotting (ESM, Fig. S1). In the bio-conjugation step, the concentration of Anti-HER2 was 100 μg/mL in D-PBS 1× at pH 7.4. The concentration of Anti-HER2* was 1 μg/mL. Since the Anti-HER2* was directly conjugated to the dye (no biotin-streptavidin recognition step), the blocking agent was SM. In all cases, the buffer was D-PBS 1× at pH 7.4, with the only exception of the cell lysates, which were diluted in a cell lysis buffer. The flow rates, the interaction times, and the working temperature were kept constant to the values quoted above.

In Fig. 6a, we show the LF sensorgram (red data points) recorded during an assay in which the 1DPC biochip interacted with a MCF-7 cell lysate. S1 is the Anti-HER2 immobilization, S2 is the blocking, S3 is the lysate interaction, and S4 is the detection. We also plot the result of an assay carried out with a 32D lysate, only in the S4 phase for the sake of clarity.

A clear binding kinetics signal is observed during S4 in the presence of MCF-7, while a flat signal appears when the 32D lysate was allowed to react with the 1DPC biochip. Moreover, such LF findings were supported by the FLUO result as depicted in Fig. 6b. In fact, the integrated fluorescence levels are well distinguished, thus demonstrating that a successful discrimination between HER2-negative and low positive cell lysates is achievable in complex biological media. Again, as experienced in the past [34], the HER2-negative cell line 32D presented a basal expression of such a biomarker when comparing its emitted intensity with the level of the blank in Fig. 6b.

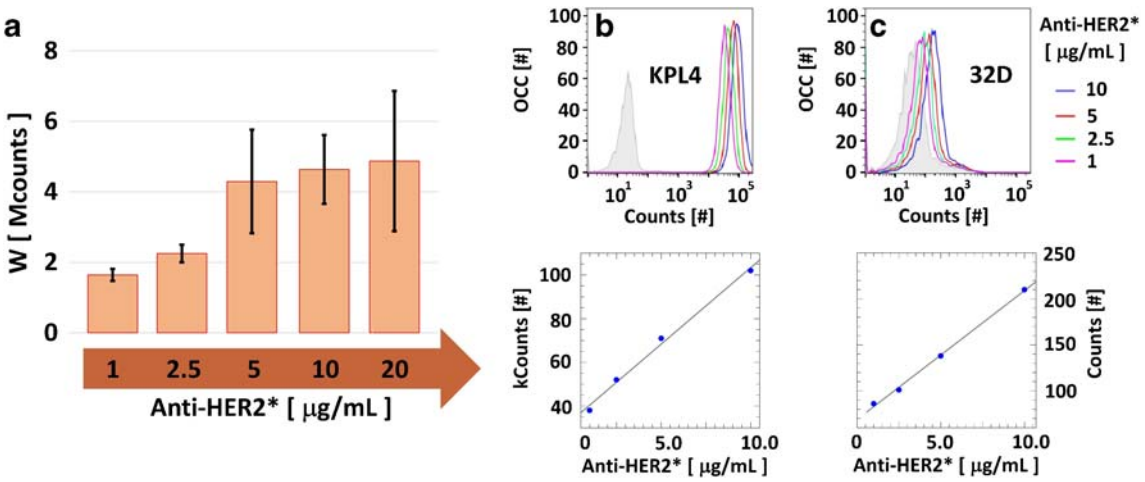

Fig. 5 (a) Integrated fluorescence intensities (W) as a function of the Anti-HER2* concentration; (b) FACS staining of 32D (HER2 negative) and KPL-4 (HER2 positive) cells with Anti-HER2*, for the indicated concentrations. The staining was repeated for different concentrations of Anti-HER2* from 1 to 10 μg/mL. The graphs below (b and c) show the counts as a function of Anti-HER2* concentrations. Shaded histograms represent the background control

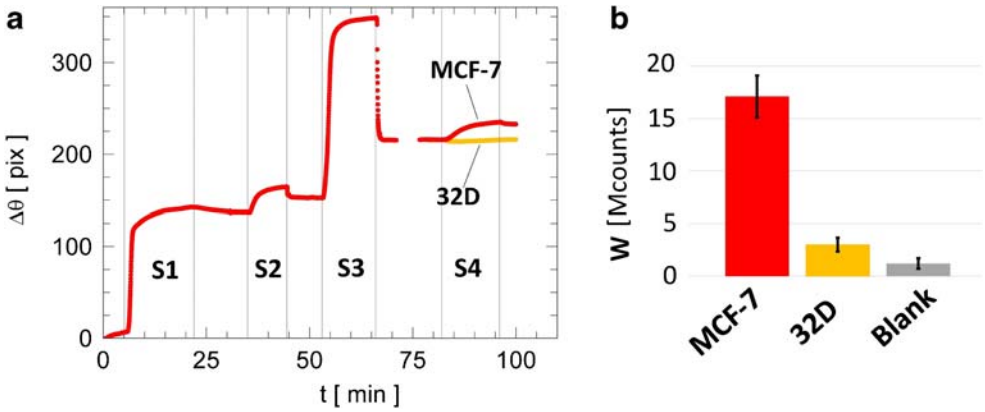

Fig. 6 (a) Complete LF sensorgrams related to a breast cancer assay for HER2 detection. The optimized assay protocol consists in four interaction steps: (S1) capture Anti-HER2 immobilization; (S2) blocking with SM; (S3) cell lysates MCF-7 (red curve) or 32D (yellow curve) interaction; (S4) detection of Anti-HER2* reported for the two cell lysates. (b) Integrated fluorescence intensities for MCF-7 (red), 32D (yellow), and the blank (gray)

Conclusions

In this work, we presented 1DPC biochips combining LF and FLUO operation modes for bioassay engineering. A modified OFAT method was used to optimize the experimental variables during bio-conjugation and detection phases to achieve an efficient HER2 bioassay. Therefore, with the aim to maximize the 1DPC biochips' response, the bio-conjugation process was studied in detail. In this case, we explored a variety of conditions: different pH of the capture antibody solution, different concentrations, different blocking agents. The multiple outcomes generated from such optimization experiments permitted us to study the capturing efficiency and the repeatability of the immobilization process that was estimated to be 6% (on 9 different 1DPC biochips). By exploiting the resolution of FLUO operation mode, we were able to study non-specific interactions for different blocking agents as well as different HER2 diluting buffers. This allowed to define the best passivation strategies, e.g., using BSA, SM, or casein, and to show that PBS 1× is appropriate as a HER2 diluting buffer. Moreover, we also addressed the issue of the concentration of the detection antibody. Following a complementary cytofluorimetric analysis, we decreased the amount of Anti-HER2* by an order of magnitude (from 10 to 1 μg/mL) to reduce FLUO background signals. Finally, we transferred all the optimized working parameters to HER2 bioassays in a complex biological environment. The LF and FLUO results obtained analyzing the MCF-7 (HER low positive) and 32D (HER negative) cell lysates demonstrated that we can successfully discriminate the two lysates providing clear advantages also in terms of duration time and consumption of small amounts of precious clinical samples [35]. The technical improvements described herein will help to develop robust HER2 detection in complex biological media and in conventional as well as novel clinical settings, particularly to monitor changes in the levels of actionable HER2 as a result of targeted therapies.

Funding information This work was funded by the Regione Lazio (TURNOFF, 85-2017-14945); by the Italian Ministry of Education, University and Research (NeoN, ARS01_00769); and by Associazione Italiana per la Ricerca sul Cancro (AIRC): Nuvenia Fellowship id. 19503 to MA; IG id. 19052 to PG.

Compliance with ethical standards

Conflict of interest The authors declare that they have no competing interests.

References

1. Armston A. The immunoassay handbook. Ann Clin Biochem. 2013;51:519–20.
2. Vashist SK, Luong JHT. Enzyme-linked immunoassays. Handbook of immunoassay technologies: approaches, performances, and applications. Academic Press; 2018. p. 19–46.
3. Yu ZTF, Guan H, Cheung MK, McHugh WM, Cornell TT, Shanley TP, et al. Rapid, automated, parallel quantitative immunoassays using highly integrated microfluidics and AlphaLISA. Sci Rep. 2015;5:11339.
4. Rizzo R, Alvaro M, Danz N, Napione L, Descrovi E, Schmieder S, et al. Bloch surface wave label-free and fluorescence platform for the detection of VEGF biomarker in biological matrices. Sensor Actuators B Chem. 2018;25(5):2143–50.
5. Kemeny DM, Challacombe SJ. ELISA and other solid phase immunoassays: theoretical and practical aspects: Wiley Medical Publications; 1988.
6. Reck M, Stahl F, Walter JG, Hollas M, Melzner D, Scheper T. Optimization of a microarray sandwich-ELISA against hINF-gamma on a modified nitrocellulose membrane. Biotechnol Prog. 2007;23(6):1498–505.
7. Sinibaldi A, Sampaoli C, Danz N, Munzert P, Sibilio L, Sonntag F, et al. Detection of soluble ERBB2 in breast cancer cell lysates using a combined label-free/fluorescence platform based on Bloch surface waves. Biosens Bioelectron. 2017;92:125–30.
8. Eletxigerra U, Martinez-Perdiguero J, Barderas R, Pingarrón JM, Campuzano S, Merino S. Surface plasmon resonance immunosensor for ErbB2 breast cancer biomarker determination in human serum and raw cancer cell lysates. Anal Chim Acta. 2016;905:156–62.
9. Montgomery DG. Design and analysis of experiments: Wiley; 2001.

10. Lye LM. Tools and toys for teaching design of experiments methodology. 33rd Annual General Conference of the Canadian Society for Civil Engineering. 2005;GC-113:1–9.
11. Ravella SR, Kumar CG, Prakasham RS, Hobbs PJ. The Taguchi methodology as a statistical tool for biotechnological applications: a critical appraisal. Biotechnol J. 2008;3(4):510–23.
12. Luo W, Pla-Roca M, Juncker D. Taguchi design-based optimization of sandwich immunoassay microarrays for detecting breast cancer biomarkers. Anal Chem. 2011;83:5767–74.
13. Mahfoud OK, Rakovich TY, Prina-Mello A, Movia D, Alves F, Volkov Y. Detection of ErbB2: nanotechnological solutions for clinical diagnostics. RSC Adv. 2014;4:3422–42.
14. Dawood S, Broglio K, Buzdar AU, Hortobagyi GN, Giordano SH. Prognosis of women with metastatic breast cancer by HER2 status and trastuzumab treatment: an institutional-based review. J Clin Oncol. 2010;28(1):92–8.
15. Page K, Hava N, Ward BJ, Brown J, Guttery DS, Ruangpratheep C, et al. Detection of HER2 amplification in circulating free DNA in patients with breast cancer. Br J Cancer. 2011;104(8):1342–8.
16. Yeh P, Yariv A, Hong CS. Electromagnetic propagation in periodic stratified media. I. General theory*. J Opt Soc Am. 1977;67(4):423–38.
17. Konopsky VN, Alieva EV. Photonic crystal surface waves for optical biosensors. Anal Chem. 2007;79:4729–35.
18. Danz N, Sinibaldi A, Michelotti F, Descrovi E, Munzert P, Schulz U, et al. Improving the sensitivity of optical biosensors by means of Bloch surface waves. Biomed Eng Biomed Tech. 2012;57:584–7.
19. Rizzo R, Alvaro M, Danz N, Napione L, Descrovi E, Schmieder S, et al. Bloch surface wave enhanced biosensor for the direct detection of angiopoietin-2 tumor biomarker in human plasma. Biomed Opt Express. 2018;9(2):529–42.
20. Munzert P, Danz N, Sinibaldi A, Michelotti F. Coatings for Bloch surface wave optical biosensors. Surf Coat Technol. 2017;314:79–84.
21. Raether H. Surface plasmons on smooth and rough surfaces and on gratings. 1st ed. Berlin: Springer; 1988.
22. Sinibaldi A, Danz N, Anopchenko A, Munzert P, Schmieder S, Chandrawati R, et al. Label-free detection of tumor angiogenesis biomarker angiopoietin 2 using Bloch surface waves on one dimensional photonic crystals. J Lightwave Technol. 2015;33(16):3385–93.
23. Rizzo R, Danz N, Michelotti F, Maillart E, Anopchenko A, Wächter C. Optimization of angularly resolved Bloch surface wave biosensors. Opt Express. 2014;22:23202.
24. Choudhury SD, Badugu R, Lakowicz JR. Directing fluorescence with plasmonic and photonic structures. Acc Chem Res. 2015;48:2171–80.
25. Lu B, Smyth MR, O'Kennedy R. Oriented immobilization of antibodies and its applications in immunoassays and immunosensors. Analyst. 1996;121:29R–32R.
26. Zhu M, Lerum MZ, Chen W. How to prepare reproducible, homogeneous, and hydrolytically stable aminosilane-derived layers on silica. Langmuir. 2012;28:416–23.
27. Walt DR, Agayn VI. The chemistry of enzyme and protein immobilization with glutaraldehyde. Trends Anal Chem. 1994;13:425–30.
28. Dai X, Cheng H, Bai Z, Li J. Breast cancer cell line classification and its relevance with breast tumor subtyping. J Cancer. 2017;8(16):3131–41.
29. Holliday DL, Speirs V. Choosing the right cell line for breast cancer research. Breast Cancer Res. 2011;13:215.
30. Giacomini P, Ng AK, Kantor RR, Natali PG, Ferrone S. Double determinant immunoassay to measure a human high-molecular-weight melanoma-associated antigen. Cancer Res. 1983;43(8):3586–90.
31. Digiesi G, Giacomini P, Fraioli R, Mariani M, Nicotra MR, Segatto O, et al. Production and characterization of murine mAbs to the extracellular domain of humanneu oncogene product GP185HER2. Hybridoma. 1992:11(4).
32. Voros J. The density and refractive index of absorbing protein layers. Biophys J. 2004;87(1):553–61.
33. Lahiri J, Isaacs L, Tien J, Whitesides GM. A strategy for the generation of surfaces presenting ligands for studies of binding based on an active ester as a common reactive intermediate: a surface plasmon resonance study. Anal Chem. 1999;71(4):777–90.
34. Sinibaldi A, Sampaoli C, Danz N, Munzert P, Sonntag F, Centola F, et al. Bloch surface waves biosensors for high sensitivity detection of soluble ERBB2 in a complex biological environment. Biosensors. 2017;7(3):33.
35. Haab BB, Dunham MJ, Brown PO. Protein microarrays for highly parallel detection and quantitation of specific proteins and antibodies in complex solutions. Genome Biol. 2001;2:1–13.